Northumbria Research Link

Citation: Oladijo, S.S., Mwema, F.M., Jen, T.C., Ronoh, Kipkurui, Sobola, Dinara and Akinlabi, Esther (2022) Nanoscale surface dynamics of RF-magnetron sputtered CrCoCuFeNi high entropy alloy thin films. Materials Today Communications, 33. p. 104523. ISSN 2352-4928

Published by: Elsevier

URL: https://doi.org/10.1016/j.mtcomm.2022.104523 <https://doi.org/10.1016/j.mtcomm.2022.104523>

This version was downloaded from Northumbria Research Link: https://nrl.northumbria.ac.uk/id/eprint/50362/

Northumbria University has developed Northumbria Research Link (NRL) to enable users to access the University's research output. Copyright © and moral rights for items on NRL are retained by the individual author(s) and/or other copyright owners. Single copies of full items can be reproduced, displayed or performed, and given to third parties in any format or medium for personal research or study, educational, or not-for-profit purposes without prior permission or charge, provided the authors, title and full bibliographic details are given, as well as a hyperlink and/or URL to the original metadata page. The content must not be changed in any way. Full items must not be sold commercially in any format or medium without formal permission of the copyright holder. The full policy is available online: http://nrl.northumbria.ac.uk/policies.html

This document may differ from the final, published version of the research and has been made available online in accordance with publisher policies. To read and/or cite from the published version of the research, please visit the publisher's website (a subscription may be required.)

Northumbria University
NEWCASTLE

CUSTOMER SERVICE EXCELLENCE CSE

UniversityLibrary

Nanoscale surface dynamics of RF-magnetron sputtered CrCoCuFeNi high entropy alloy thin films

S.S. Oladijo[1], F.M. Mwema[1,2], T.C. Jen[1], Kipkurui Ronoh[2,3], Dinara Sobola[4,5], E.T. Akinlabi[6]

[1] Department of Mechanical Engineering Science, University of Johannesburg
[2] Department of Mechanical Engineering, Dedan Kimathi University of Technology, Private Bag-10143, Dedan Kimathi, Nyeri, Kenya
[3] Central European Institute of Technology, Brno University of Technology, Purkyňova 123, 612 00 Brno, Czech Republic
[4] Department of Physics, Faculty of Electrical Engineering and Communication, Brno University of Technology, Technická 2848/8, 616 00 Brno, Czech Republic
[5] Institute of Physics of Materials, Czech Academy of Sciences, Žižkova 22, 61662 Brno, Czech Republic
[6] Department of Mechanical and Construction Engineering, Northumbria University, Newcastle, NE1 8ST. United Kingdom

Abstract

High entropy alloy (HEA) thin films of CrCoCuFeNi are grown on stainless steel substrate using radiofrequency (RF) magnetron sputtering method at different sputtering times (30, 60 and 90 minutes), substrate temperatures (room temperature, 100 and 200 deg. Celsius) and RF powers (100, 150 and 200 W). The nanoscale morphology and topography of the thin films are obtained using an atomic force microscopy (AFM) method. The average surface roughness, interface width, fractal and multifractal characteristics of the films are presented. It is shown that the average surface roughness and interface width decrease with the time of deposition while considering the combination of the other factors. The autocorrelation and height-height correlation functions reveal that these surfaces are self-affine and exhibit fractal characteristics. The increase in sputtering power, with different combinations of time and temperature, is related to large fractal dimension and small lacunarity coefficient. The increase in substrate temperature (for different combinations with time and RF power) is shown to enhance the spatial roughness of the HEA thin films. A multifractal analysis undertaken using generalized fractal dimension, mass exponent against moment order and multifractal spectrum reveal that all the films have a multifractal character; and the films deposited at high temperatures and powers exhibit the strongest multifractal behaviour.

Keywords: *High entropy alloy thin films; fractals; surface roughness; sputtering; fractal dimension; Lacunarity; multifractal*

1 Introduction

High entropy alloy (HEAs) thin films have attracted a lot of interest among researchers due to the attractive attributes they offer in terms of properties and applications [1]. In definition, HEAs are alloys with at least five different components and a mole percentage from each element ranging from 5% to 35%. In terms of thermodynamics, HEA films are more likely to form multi-element solid-solution phases rather than the complicated intermetallic compounds due to the enhanced mixing entropy impact caused by the increased number of significant component elements [2]. As such, HEAs films have several unique properties, including high hardness, wear and corrosion resistance, excellent thermal stability, high strength and ductility, superior stability to irradiation, excellent fatigue and oxidation resistance [3].

Due to the attractive properties, several studies have been conducted on properties and characterization of HEA coatings and thin films. Sha et al. used the direct current (DC) magnetron sputtering technique to deposit FeMnNiCoCr HEA coatings, demonstrating remarkable ductility and strength [4]. Liang et al. investigated AlCoCrFeNi HEA coatings and demonstrated that HEA coatings exhibit excellent stability for high temperature applications [5]. Khan et al. [6] investigated the significant magnetron sputtering parameter that can be optimized to tune the physical and chemical properties of HEA thin films for applications; they demonstrated that sputtering radiofrequency (RF) power is key in regulating the composition and microstructure of HEA thin films. The results show that increasing power improves the hydrophobicity, and alters the composition and microstructure of HEA thin films, allowing for fine-tuning of their physical properties. Sha et al. [7] investigated the effect of the addition of nitrogen (N) element to FeMnNiCoCr HEA on the microstructural growth, tribological, and mechanical properties. It was revealed that the coatings with low nitrogen N content exhibit an FCC structure, which provides the best adhesion strength and scratch toughness but lowers wear resistance and hardness. Thin films with medium N content have a BCC structure, which improves wear resistance and hardness but reduces the scratch responses. Coatings with a higher N nitrogen content have an impressive combination of superior wear resistance and hardness, good scratch response, and have a well-defined structure. These BCC grains and N-reinforced grain borders overcome the contradiction between ductility and strength. An investigation by Wang et al. on the tribo-mechanical properties of sputtered CrNbTiMoZr HEAs film reveals the films' exceptional tribological properties [8].

It is no doubt that studies on high entropy alloy (HEA) thin films are very scanty; this is due to the fact that HEA is still a developing area, holistically. In addition, most of the existing HEA thin film studies focus on their mechanical properties and performance in conditions of wear and corrosion. In fact, there are very few studies focusing on the scaling behaviour of HEA thin films during a typical thin film deposition process. Studies into the nanoscale dynamics of such films are necessary for advancing the deposition processes for excellently-tuned HEA thin films for high performance applications. In this study, therefore, and for the first time ever, nanoscale dynamic analyses, through fractal and multifractal methods, are used to understand the surface evolution during sputtering of solid CoCrCuFeNi HEAs thin films deposited on stainless steel 304 using radio frequency magnetron sputtering. The films were deposited at carefully selected combination of the deposition parameters of the substrate temperature, deposition time, and RF power. The research will advance knowledge on the evolution of surface structures during the deposition of HEA thin films such as CoCrCuFeNi films.

2 Methods

Using an HHV TF500 RF magnetron sputtering thin film coatings system, deposition of a high entropy alloy target consisting of $Co_{17.8}$, $Cr_{21.6}$, Cu_{23}, $Fe_{18.5}$, $Ni_{19.1}$ at% was undertaken on the stainless steel substrate. The deposition was undertaken at different sputtering times, power, and substrate temperatures. The sputtering system's descriptions and procedure have already been described in the published literature [9–11]. Before mounting the substrates into the substrate holder inside the sputtering chamber, the commercially available stainless steel 304 substrates were cleaned and polished to a mirror finish. To reduce residual oxygen for all the depositions, the chamber was first pumped down to a base pressure of 5.0×10^{-5} mbar. The substrate holder rotated at a constant speed of 5 rpm. The target and substrate holder were separated by a set working distance of 150 mm. Pre-sputtering was done for a few minutes to clean the surface of the target, while the argon gas flowrate was kept at 14 standard cubic centimetres per minute (sccm). Samples were prepared at different conditions of time, power and temperature as illustrated in Table 1. The parameters used in the process have been succesfull in preparing quality thin films of the material in our laboratory.

Table 1 Magnetron sputtering conditions of high entropy alloy (CrCoCuFeNi) thin films

Sample Description	**Deposition parameters**		
	Time (mins)	**Sputtering power (W)**	**Substrate temperature (^{o}C)**
A	30	100	RT
B	30	150	200
C	30	200	100
D	60	100	200
E	60	150	100
F	60	200	RT
G	90	100	100
H	90	150	RT

The obtained samples were characterized for surface topography using Atomic Force Microscope (AFM) (Dimension Icon®, Bruker). It is a technique that can display any vertical changes on the surface of the film with a resolution of up to 0.1 nm [12, 13]. The samples were examined in ScanAsyst-Air mode as this mode is easier and faster to get consistent, high-quality results and do not harm the thin metallic films. A silicon carbide cantilever probe with a nominal thickness of 0.5µm, and tip specifications were a height of 5 µm and thickness of 2 nm was used. The spring constant of the cantilever was 0.400 N/m. A scan angle of 0.00°, a scan rate of 1 Hz, a peak tapping force amplitude of 150 nm and peak frequency of 2 kHz. The surface topographies of the thin film samples were obtained by scanning over a 1 µm × 1 µm area with a resolution of 1024 x 1024 pixels. The imaging was undertaken at ambient conditions of relative humidity of 50% and room temperature of 25°C. Ten images were obtained for each surface sample to obtain a representative average of the analysis parameters.

Gwyddion software, a free and open-source software, was used for data visualization and image analysis [14]. Baseline correction of the AFM images was done using align rows command using the Polynomial 4 method. A statistical analysis of the thin films to determine their stereometric characteristics was undertaken on *Gwyddion* software according to ISO 25178-2:2021 [15]. These features include moment-based such as interface width (root mean square roughness), mean roughness, kurtosis and skewness; order-based such as maximum peak height, maximum pit depth, and a maximum height of features and; hybrid properties such as that inclination, variation and surface slope. Other features include height distribution histograms and surface texture plots.

In addition, fractal behaviour was evaluated through fractal dimension and multi-fractal characterisation using *FIJI* (formerly known as *ImageJ*) with *FracLac* plug-in for fractal analyses. A complete methodology for the analyses has been extensively presented in the literature by the authors of this article [16] and other researchers [17, 18].

3 Results and Discussion

Figure 1 represents 3D AFM topography maps of the CrCoCuFeNi thin films deposited on stainless steel substrates. It can be observed that films deposited at low deposition times, i.e., 30 minutes (A, B, and C) exhibit well-developed grain structures whereas those obtained at 90 minutes (G and H) of sputtering exhibit highly interconnected grain structures. It can also be deduced that HEAs thin films grown at room temperature, RT (°C) have large surface grains with sharp-pointed peaks and pits. In particular, samples A, F and H have sharp and large surface grains and visible pits on their surfaces. Thin films deposited at high temperatures are shown to exhibit finer grains with less surface pits and better surface coverage (samples B and D). The influence of sputtering power on grain evolution is not clear in these results, although, it can be deduced that films prepared at high powers and high temperatures exhibit large surface structures (e.g., samples C and E).

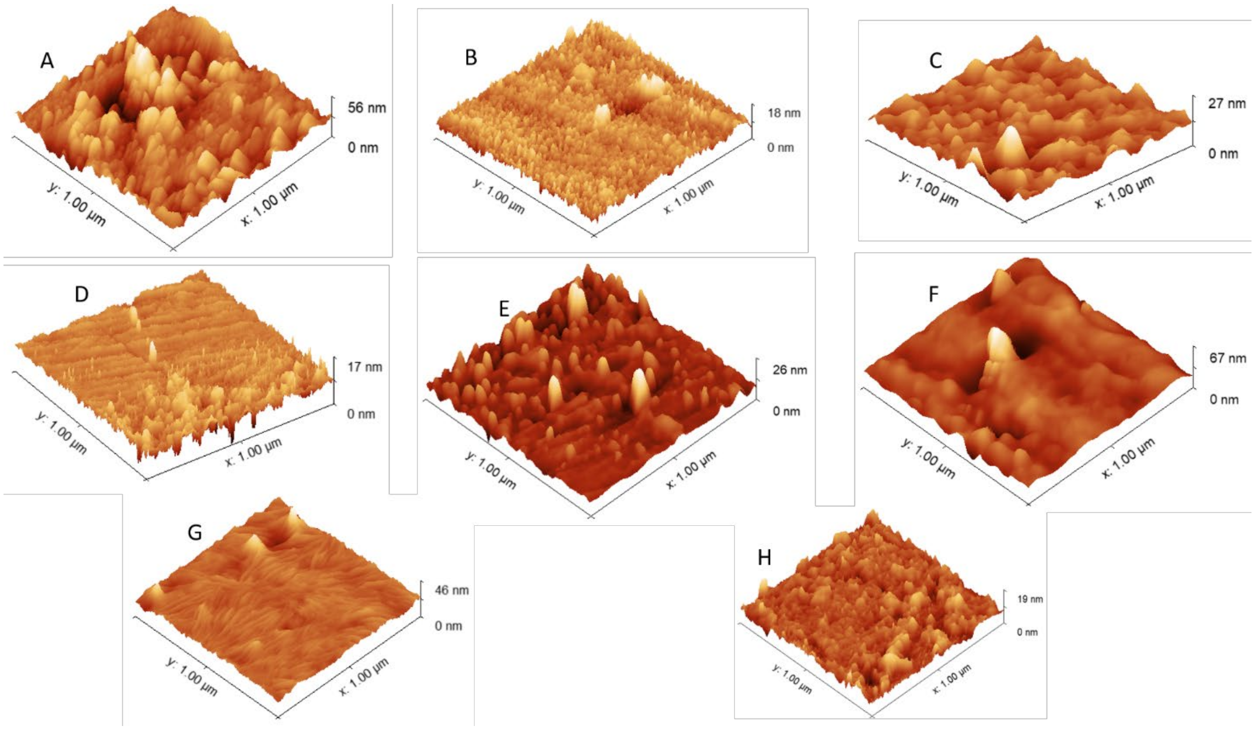

Figure 1. 3-D Atomic force microscopy (AFM) images for CrCoCuFeNi high entropy thin films sputtered on stainless steel

The density distribution histograms corresponding to the topography maps in Figure 1 are shown in Figure 2 including the Gaussian function fitting. These histograms are the representation of the peak counts against the height of peaks; the peak count implies the number of peaks per unit length whereas the peak height is the vertical deviation of the maximum points from the mean height of surface features. The general indicatation of these results is that the lowest average peak height from the distribution is ~ 10 nm with a maximum peak height of ~ 65 nm. The histograms further show that structures in samples B, C, D, G and H exhibit an accurate Gaussian distribution with one strong peak and several weak peaks (not shown). The strong peak (depicting a nearly unimodal structure) is an indication of less heterogeneity in the structures. It also indicates a better surface coverage of the coating onto the substrate. This is very important especially for protective thin films/coatings such as these HEA thin films. All the histograms exhibit near bell-shaped profiles and are tall and narrow, indicating a small standard deviation of the distribution of the surface peaks. However, the histograms for samples A and F are slightly shorter and wider compared to the rest of the samples, which indicates a larger standard deviation of the distribution of the sizes of the surface peaks. These histograms (with Gaussian function fits) are a depiction of statistical surface roughness and uniformity of surface structures of the thin films.

The statistical surface roughness characteristics of the samples were computed based on existing equations [19] and represented in Table 2. From the table, it is evident that surface roughness (both interface width and average) generally decreases with deposition time. It is also shown that films deposited at room temperature, generally, exhibit the highest surface roughness (A, F and H). Thin films grown at 200°C can be seen to exhibit the lowest surface roughness (e.g. samples B and D). The radiofrequency sputtering power does not exhibit a predictable relationship with the surface roughness of the deposited thin films. Similar observations were reported for aluminium thin films prepared on the same sputtering facility [9] and the contrary for Ti thin films prepared via DC magnetron sputtering [18]. It implies therefore sputtering power is a subject for process optimization in further studies and scienfitic representation of the influence of sputtering power on surface roughness characteristics. The samples deposited at room temperature (e.g. A and F) show the largest values of maximum peaks and pit depths. The values for skewness, for all the samples, except for sample D, are positive, which agrees with the histograms and Gaussian function fitting in Figure 2. The negative values for D indicate that the surface is nearly a perfect Gaussian function (since its kurtosis and skewness values are very close to 3 and zero respectively) and exhibits the tallest and narrowest histogram profile. The coefficient of kurtosis, generally, increases with the deposition time and it is highest on samples deposited at high substrate temperatures (e.g. samples G and E). It means that as the deposition time and temperature increase there is the formation of bumpy surfaces of the thin films.

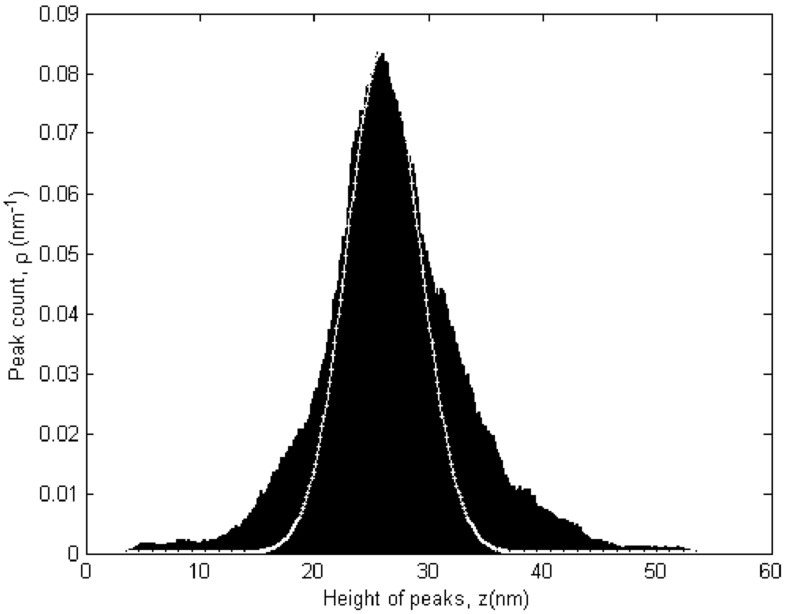
Peak count, ρ (nm^{-1})
Height of peaks, z(nm)
0.09
0.08
0.07
0.06
0.05
0.04
0.03
0.02
0.01
0
0
10
20
30
40
50
60

A

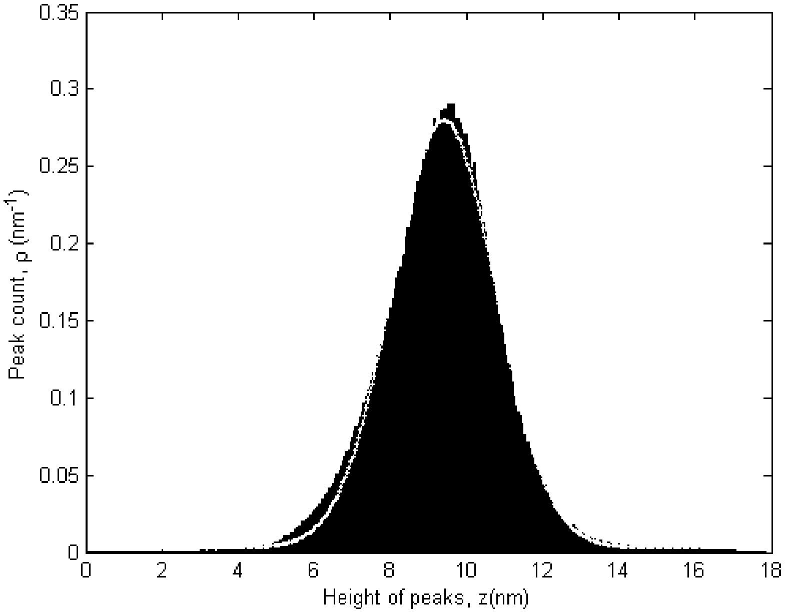
Peak count, ρ (nm^{-1})
Height of peaks, z(nm)
0.35
0.3
0.25
0.2
0.15
0.1
0.05
0
0
2
4
6
8
10
12
14
16
18

B

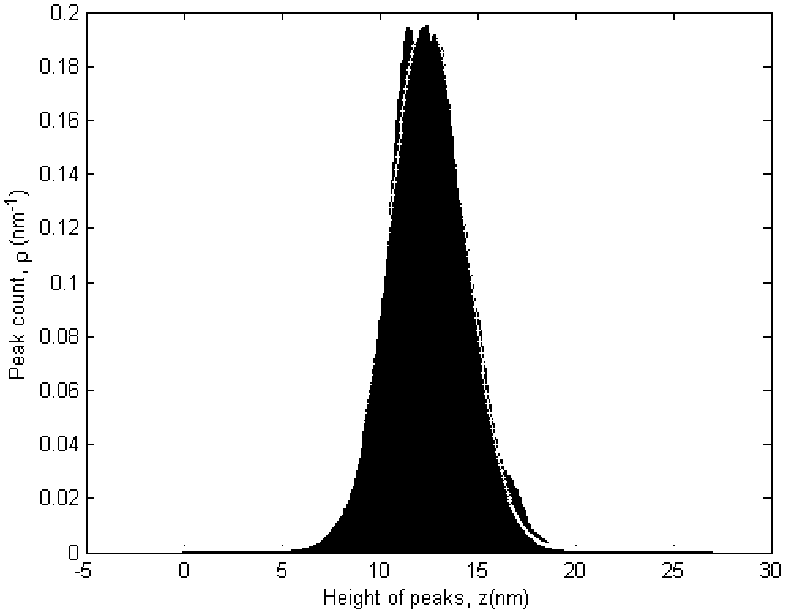
Peak count, ρ (nm^{-1})
Height of peaks, z(nm)
0.2
0.18
0.16
0.14
0.12
0.1
0.08
0.06
0.04
0.02
0
-5
0
5
10
15
20
25
30

C

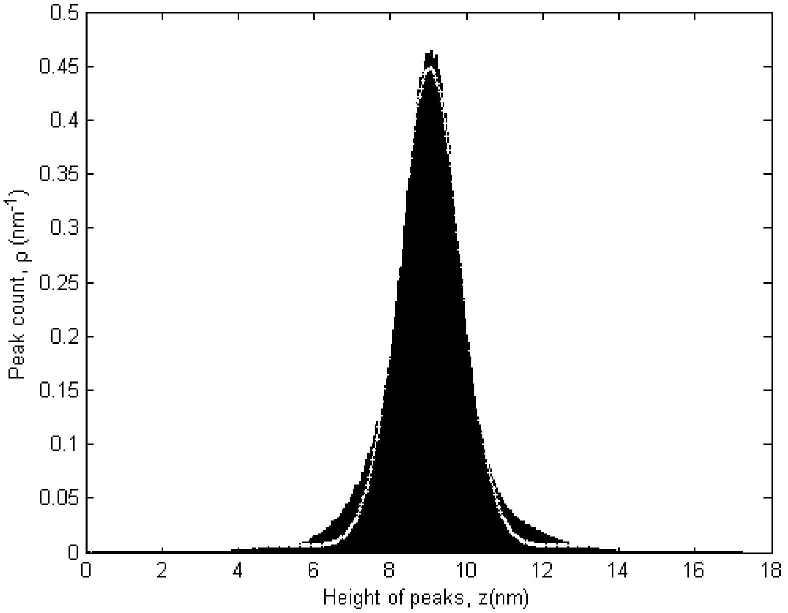
Peak count, ρ (nm^{-1})
Height of peaks, z(nm)
0.5
0.45
0.4
0.35
0.3
0.25
0.2
0.15
0.1
0.05
0
0
2
4
6
8
10
12
14
16
18

D

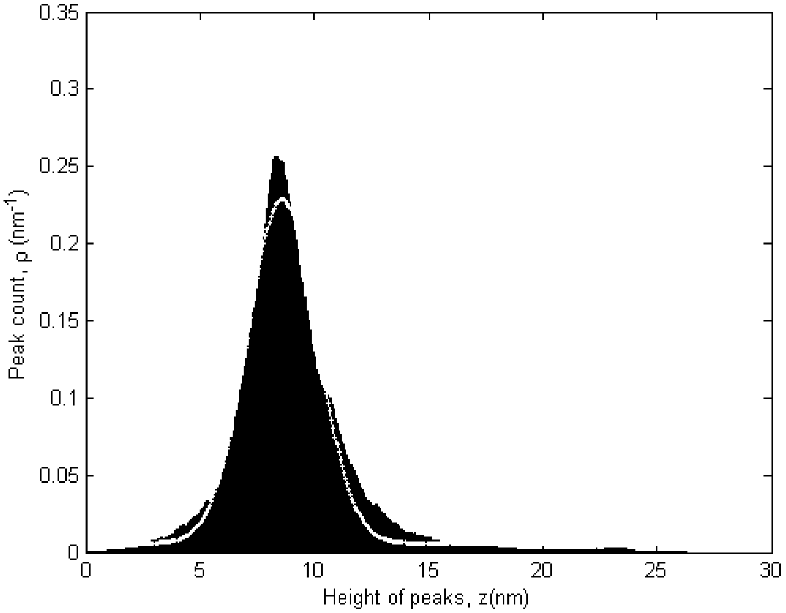

0.35
0.3
0.25
0.2
0.15
0.1
0.05
0
Peak count, ρ (nm^{-1})
0
5
10
15
20
25
30
Height of peaks, z(nm)

E

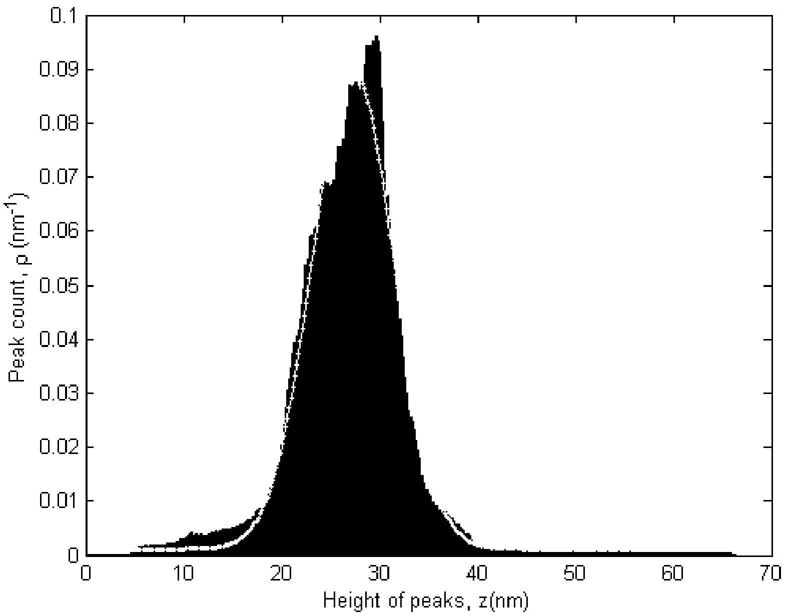

0.1
0.09
0.08
0.07
0.06
0.05
0.04
0.03
0.02
0.01
0
Peak count, ρ (nm^{-1})
0
10
20
30
40
50
60
70
Height of peaks, z(nm)

F

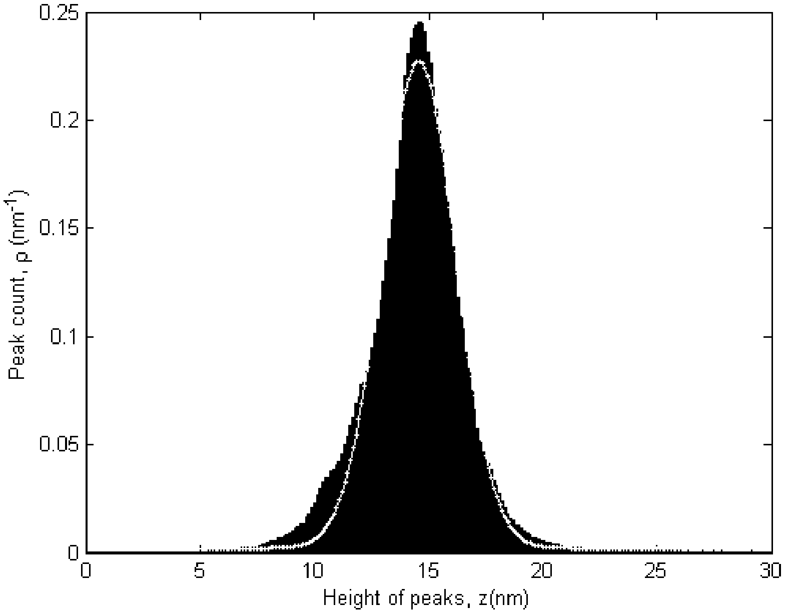

G

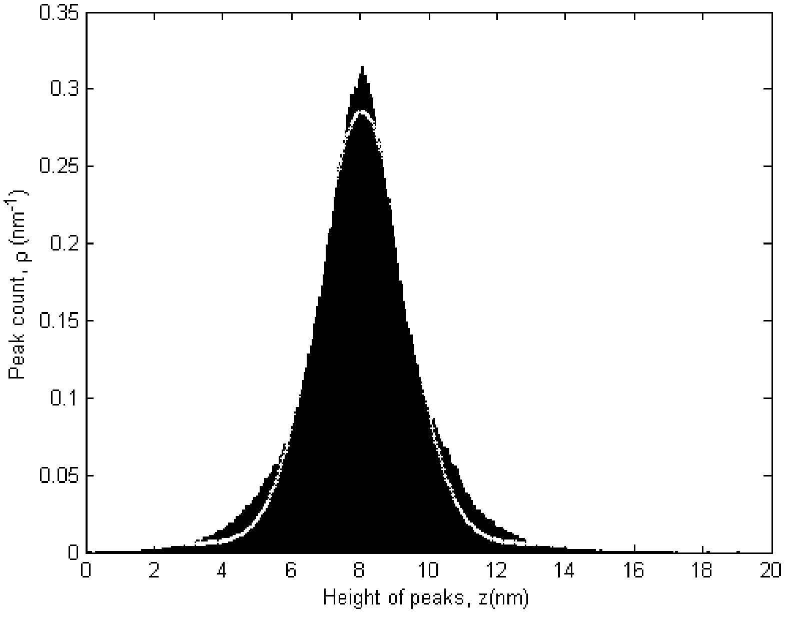

H

Figure 2. The peak count histograms showing the height distribution of peak count per unit length (ρ) against the peak height (z) for sputtered thin films A, B, C, D, E, F, G, and H. The continuous white line represents the Gaussian function fit to the data.

Table 2 Computed values of the surface roughness parameters of the sputtered thin films

Sample	**Average roughness Ra (nm)**	**Interface width w (nm)**	**Lateral correlation, ε (nm)**	**Maximum peak height, Sp (nm)**	**Maximum pit depth, Sv (nm)**	**Maximum height, Sz (nm)**	**Skew Ssk**	**Kurtosis**	$\gamma = \frac{log w}{log \varepsilon}$
A	4.82	6.50	0.036	28.71	26.99	55.70	0.25	1.48	-0.56
B	1.22	1.62	9.73	8.52	9.39	17.90	0.19	1.88	0.21
C	1.73	2.37	29.12	14.43	12.63	27.6	0.60	4.63	0.26
D	0.84	1.16	13.38	8.23	9.04	17.27	-0.11	3.31	0.06
E	1.79	2.63	24.43	17.32	9.05	26.37	1.58	6.56	0.30
F	4.16	6.00	39.68	39.42	27.11	66.53	0.67	6.15	0.49
G	1.65	2.45	38.53	28.33	14.54	42.86	1.60	15.73	0.25
H	1.25	1.68	18.98	11.00	8.11	19.11	0.10	1.35	0.18

As mentioned in literature [20], average surface roughness and interface width are global parameters and they only provide information on the vertical deviation of surface features; they do not provide information on local roughness, lateral evolution and correlations of the surface features. Fractal tools such as autocorrelation (A(r)) and height-height (H(r)) correlation functions are employed to study these properties and are shown in Figures 3 and 4. The plots of A(r) show an exponentially decreasing behaviour, which indicates that all the surfaces exhibit self-affine fractal character. It can also be seen that samples such as F and G exhibit significant oscillatory behaviour, which indicates that the surfaces of these samples are mounded. The formation of the mounded surfaces may be attributed to the clustering of structures at high sputtering power and substrate temperature. From A(r) plots, the lateral correlations were determined, as can be observed in Table 2, and it is clear that sample A (prepared at the lowest time, 100 W and RT) exhibits the smallest length, indicating that it exhibits the highest lateral roughness. Despite having very high average surface roughness, samples F and G, exhibit very large lateral correlation length, indicating low lateral surface roughness across their surface.

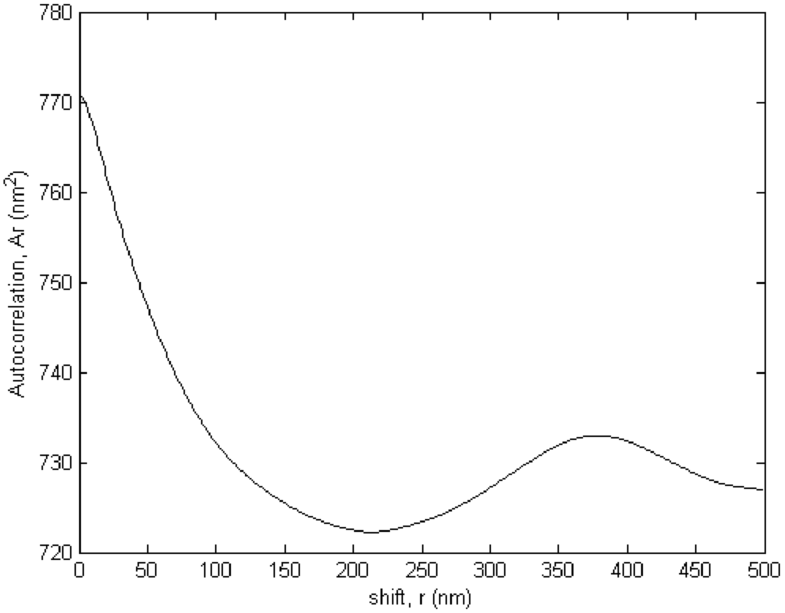
780
770
760
750
740
730
720
0
50
100
150
200
250
300
350
400
450
500
Autocorrelation, Ar (nm^2)
shift, r (nm)

A

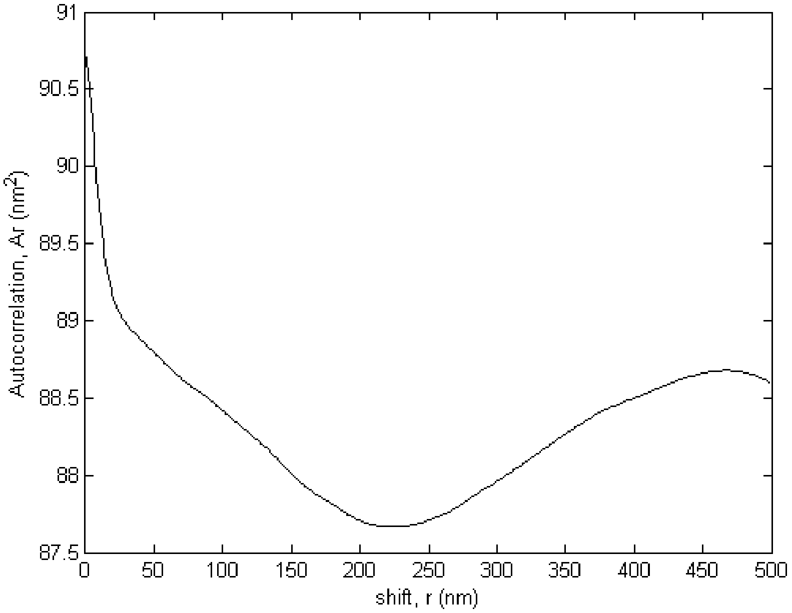
91
90.5
90
89.5
89
88.5
88
87.5
0
50
100
150
200
250
300
350
400
450
500
Autocorrelation, Ar (nm^2)
shift, r (nm)

B

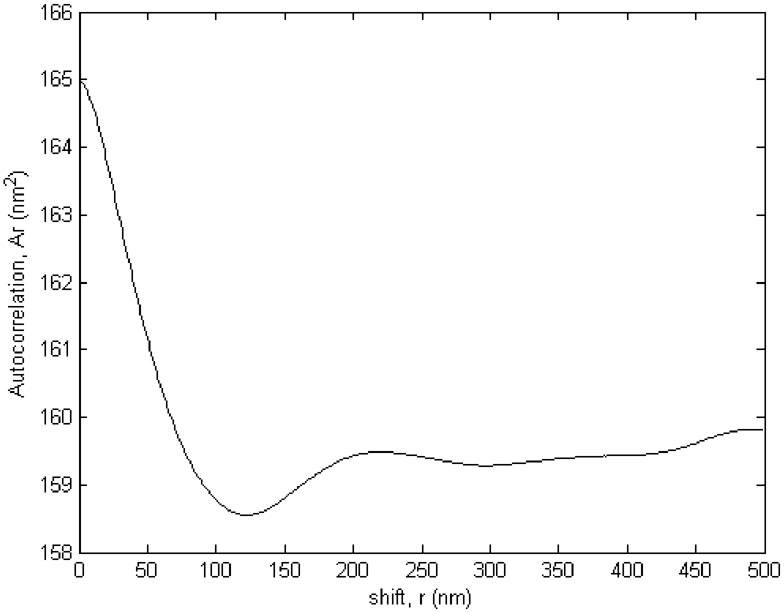

166
165
164
163
162
161
160
159
158
Autocorrelation, Ar (nm^2)
0
50
100
150
200
250
300
350
400
450
500
shift, r (nm)

C

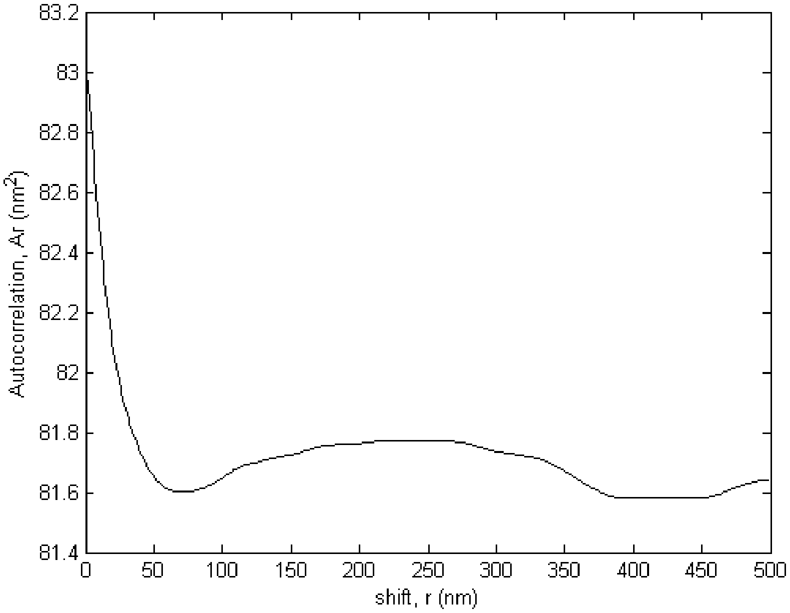

83.2
83
82.8
82.6
82.4
82.2
82
81.8
81.6
81.4
Autocorrelation, Ar (nm^2)
0
50
100
150
200
250
300
350
400
450
500
shift, r (nm)

D

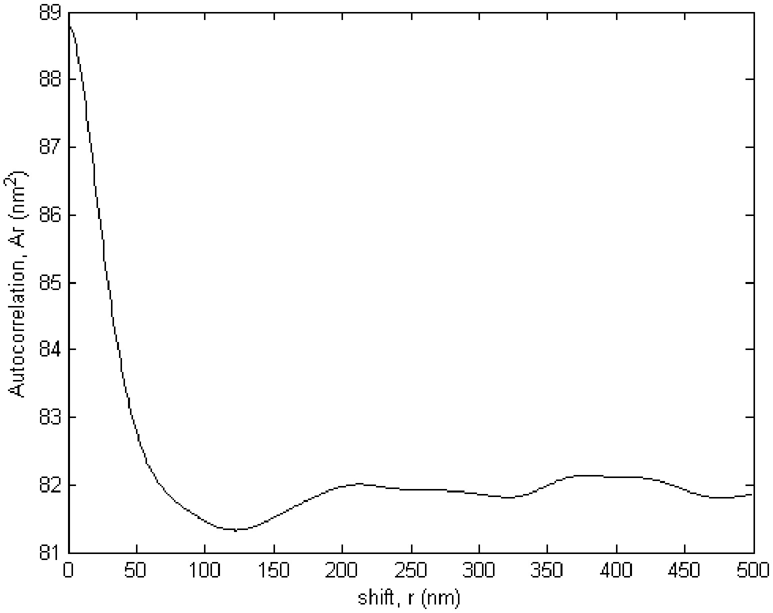
89
88
87
86
85
84
83
82
81
Autocorrelation, Ar (nm^2)
0
50
100
150
200
250
300
350
400
450
500
shift, r (nm)

E

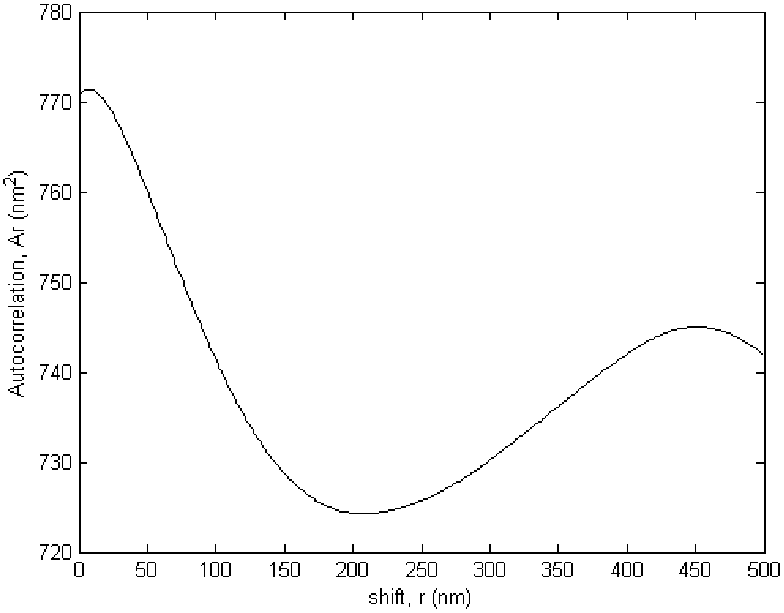
780
770
760
750
740
730
720
Autocorrelation, Ar (nm^2)
0
50
100
150
200
250
300
350
400
450
500
shift, r (nm)

F

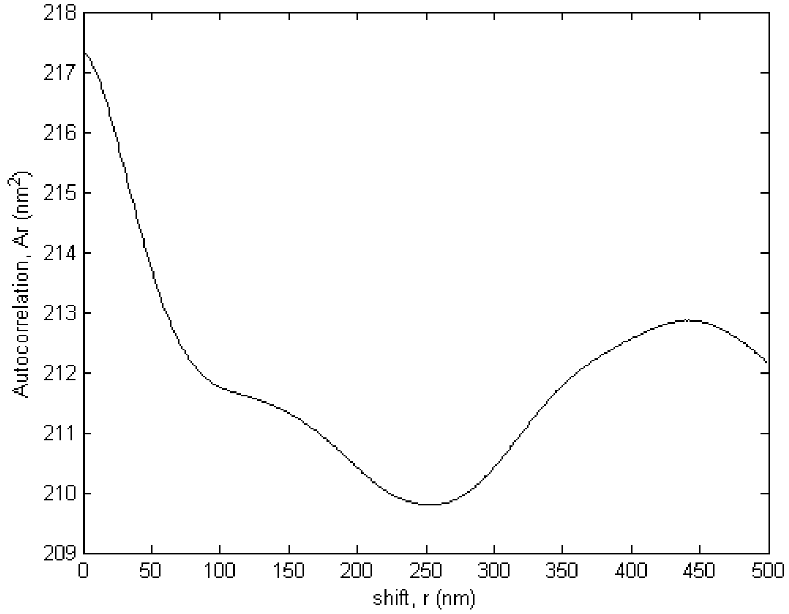

G

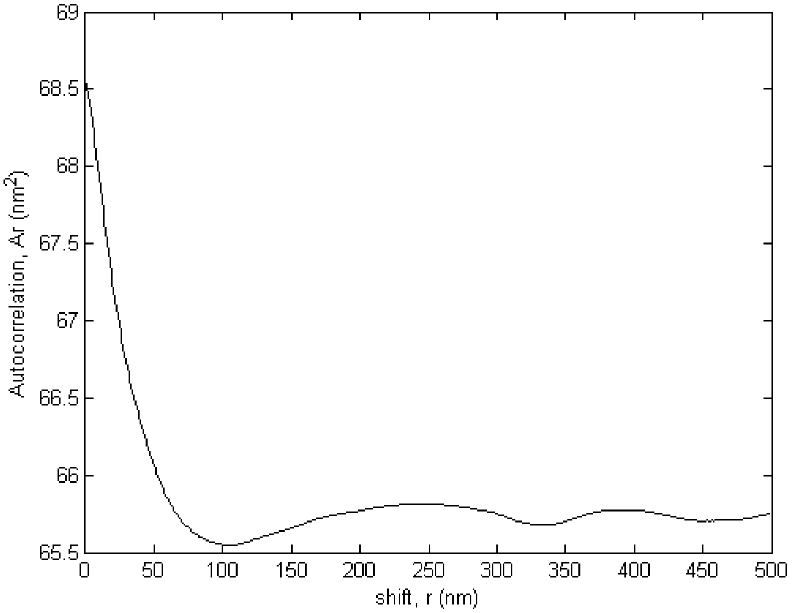

H

Figure 3. Graphical representation of autocorrelation functions of high entropy alloy films A, B, C, D, E, F, G and H sputtered on the stainless steel substrate.

The height-height correlation functions representations for the samples are shown in Figure 4. This technique determines the lateral properties based on power differences between points on various surfaces of structures. As shown, the function exhibits two regimes for all the samples; at small values of r, there is linear behaviour of the function indicating the scaling character of the films whereas at large values of r the plots exhibit nonlinear and oscillatory characteristics. These characteristics of the H(r) profile indicate self-affine surfaces. At larger r, there occurs saturation at $2\omega^2$. These properties have been related to Gaussian noise attributed to the shadowing effect due to roughening effect of Kardar-Parisi-Zhang (KPZ) non-linearity. The shadowing effect results in the growth of taller surfaces with a high sticking coefficient at the expense of the shorter ones. This leads to the formation of mounded surfaces as depicted by the 3D topography AFM maps. As shown in Table 2, the computed values of γ are less than unity, which shows a faster rate of evolution of structures in the spatial direction.

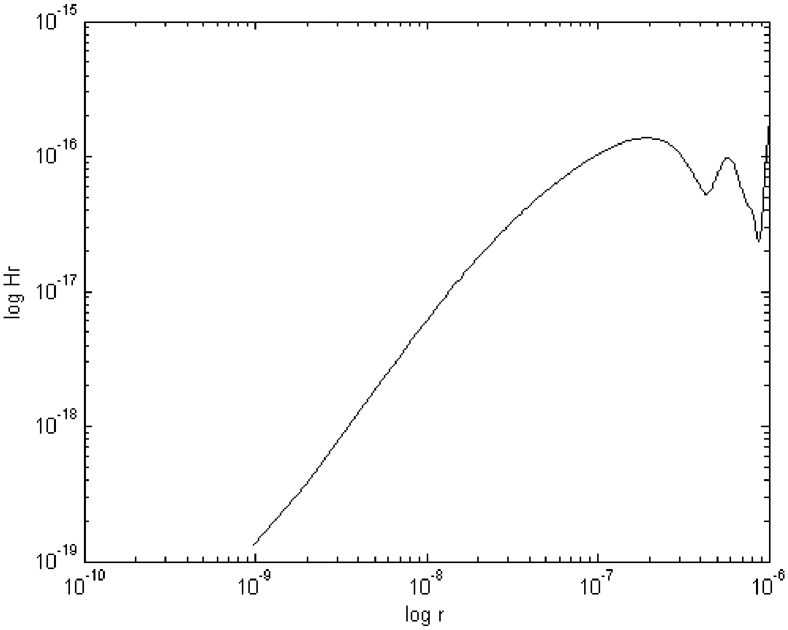

A

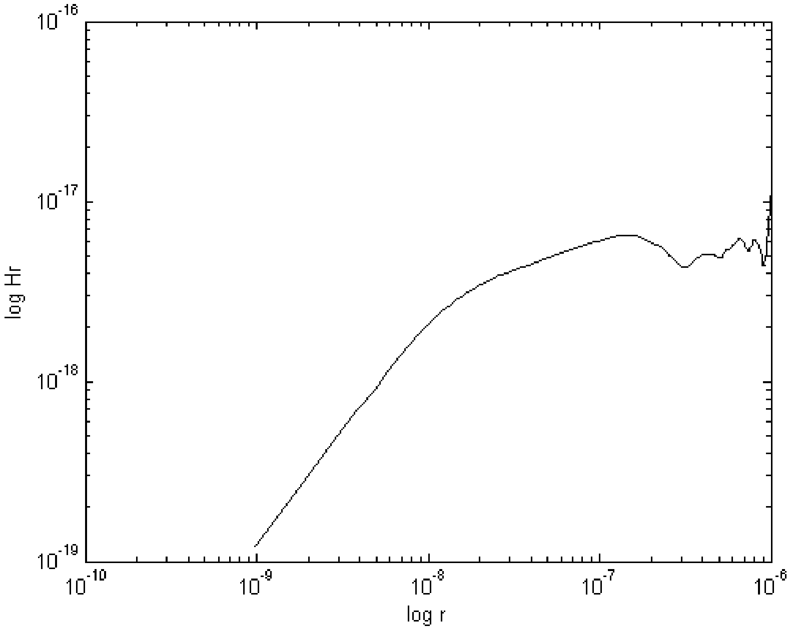
10^{-16}
10^{-17}
10^{-18}
10^{-19}
log Hr
10^{-10}
10^{-9}
10^{-8}
10^{-7}
10^{-6}
log r

B

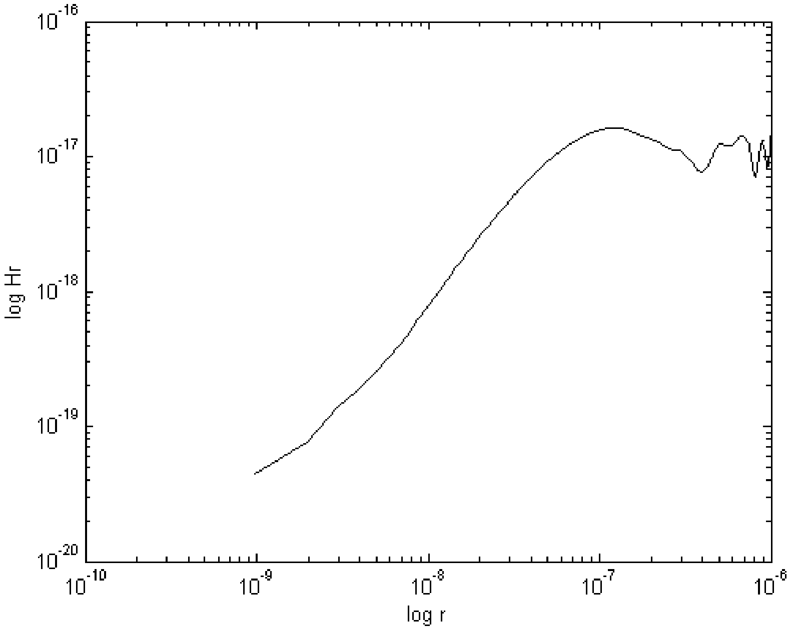
10^{-16}
10^{-17}
10^{-18}
10^{-19}
10^{-20}
log Hr
10^{-10}
10^{-9}
10^{-8}
10^{-7}
10^{-6}
log r

C

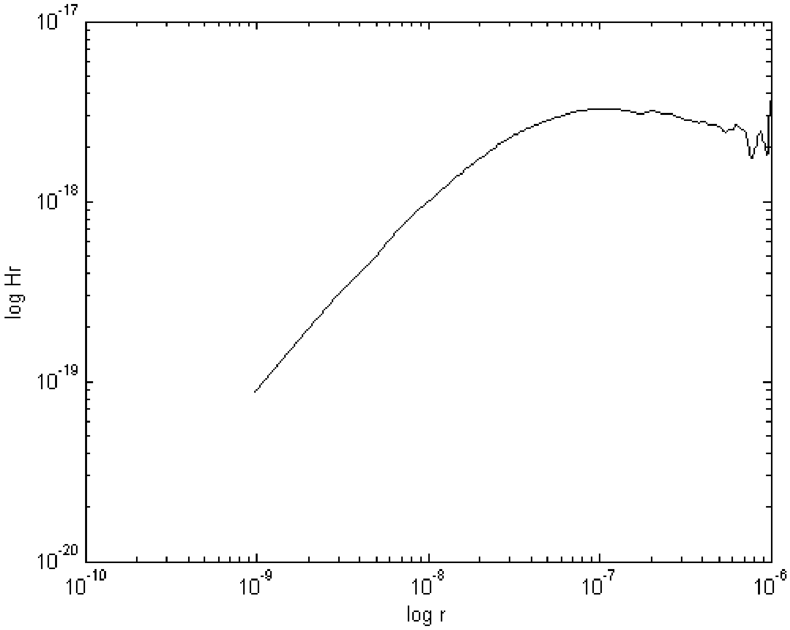
10^-17
10^-18
10^-19
10^-20
log Hr
10^-10
10^-9
10^-8
10^-7
10^-6
log r

D

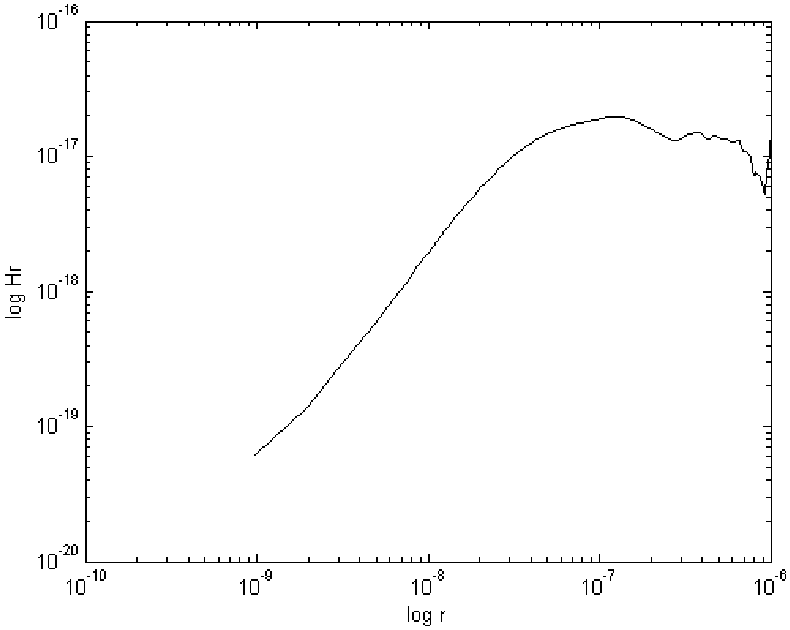
10^-16
10^-17
10^-18
10^-19
10^-20
log Hr
10^-10
10^-9
10^-8
10^-7
10^-6
log r

E

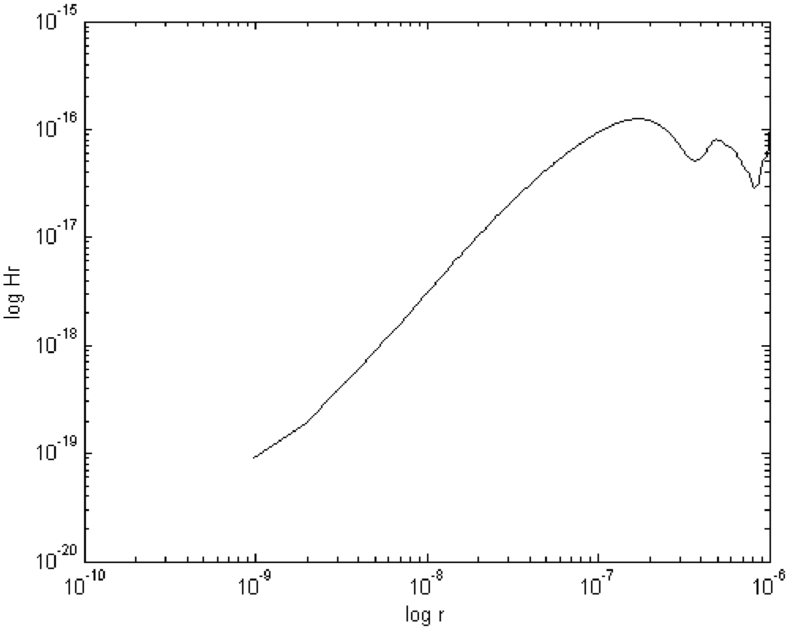

10^-15
10^-16
10^-17
10^-18
10^-19
10^-20
log Hr
10^-10
10^-9
10^-8
10^-7
10^-6
log r

F

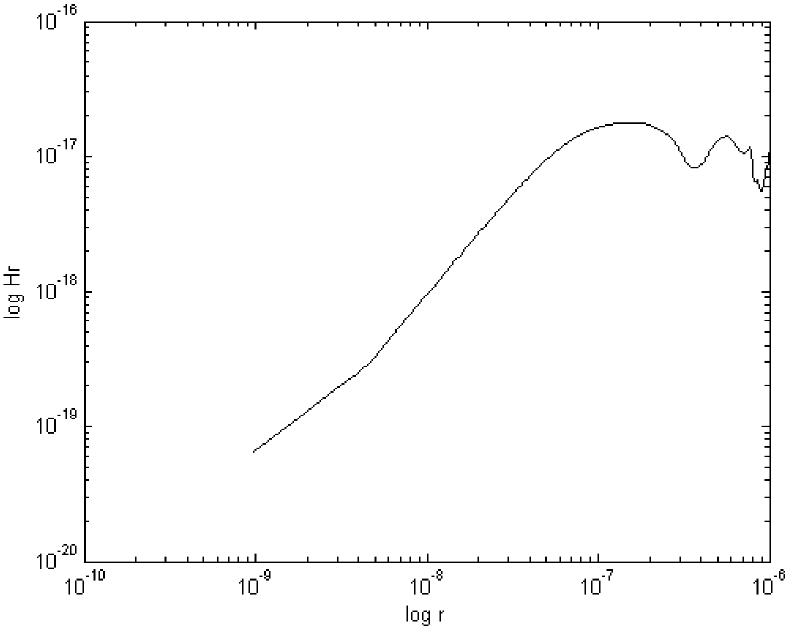

10^-16
10^-17
10^-18
10^-19
10^-20
log Hr
10^-10
10^-9
10^-8
10^-7
10^-6
log r

G

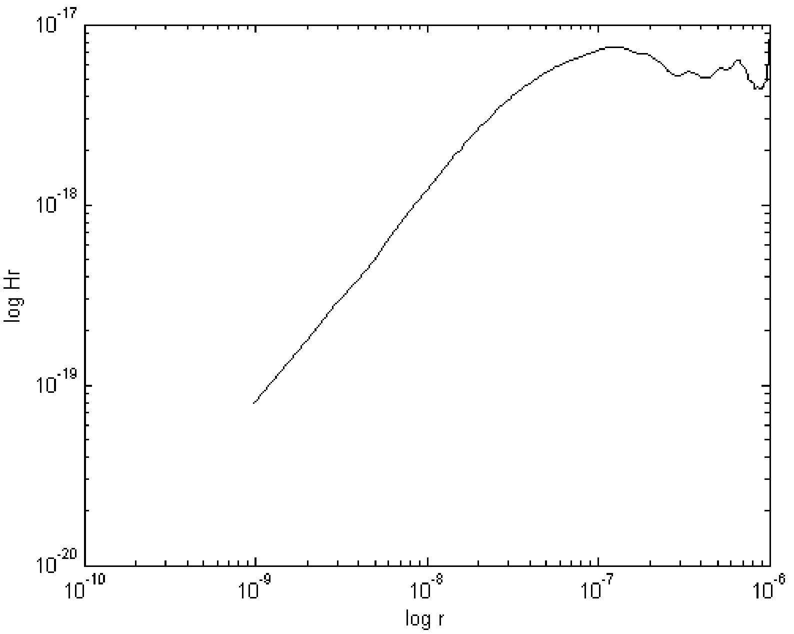

H

Figure 4. Graphical representation of height-height correlation function of CrCoCuFeNi thin films A, B, C, D, E, F, G and H sputtered on stainless steel substrates

The fractal characteristics in terms of the fractal dimension and lacunarity coefficient for the samples are represented in Table 3. The fractal dimensions were obtained from the height-height correction functions using a procedure described in our publications [21] whereas the coefficient of lacunarity was computed through a linear fit on a plot of log (lacunarity) versus log (size of grid of the box-counting method) as described by Das et al. [18]. For all the samples, the fractal dimensions indicate low spatial complexities ($D_f<2.5$). The coefficients of lacunarity indicate gaps in the structure or the non-uniformity of the surface structures; it can be seen that samples C, H and D (prepared at sputtering power above 100 W) exhibit the lowest values. This indicates that an increase in sputtering power enhances the uniform spatial distribution of surface structures during sputtering. Samples B and D exhibit the highest fractal dimensions; this indicates that an increase in substrate temperature results in an increase in spatial complexity of the grown HEAs thin film materials. There is no clear relationship between the values of the fractal dimension and the deposition time (Table 3).

The plots of generalized fractal dimension versus moment (Figure 5) exhibit a non-linear decreasing behaviour with a sigmoidal character at q=0, that indicates that all the surfaces are multifractal. It is also clear that for all the samples, $D_f(0) > D_f(1) > D_f(2)$ is true, which confirms the multifractal nature of these films. As such, the films' structure can be described by the three dimensions, i.e. capacity dimension (q=0), information dimension (q=1) and correlation dimension (q=2) as shown in Figure 5. As expected, samples with higher complexity (deposited at high temperature), such as B and D, have their profiles shifting upwards as compared to the rest of the samples. The multifractal nature of these films can be confirmed by the scaling exponent, $\tau(q)$, versus moment order, q in Figure 6. The profile exhibits a non-linear relationship with modulation at q=0, a multifractal characteristic.

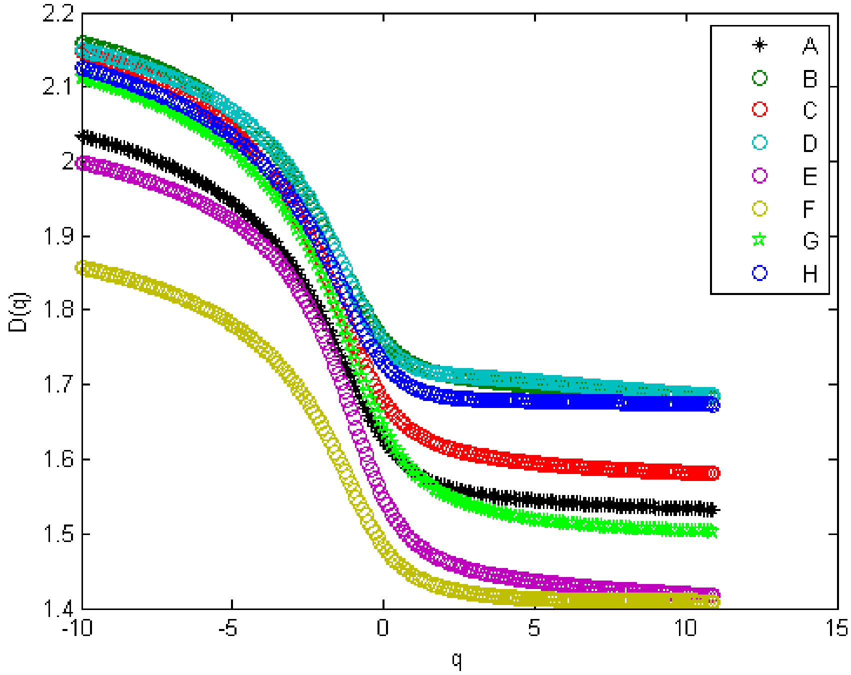

Figure 5. Generalized fractal dimension $D_f(q)$ versus moment (q) of the sputtered CrCoCuFeNi thin films

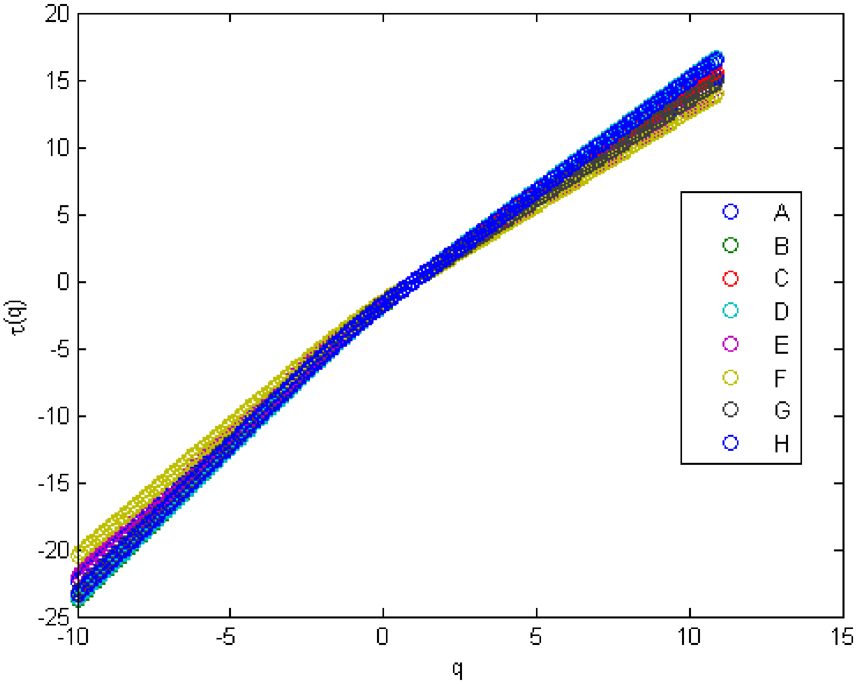

Figure 6. Mass exponent $\tau(q)$ versus moment (q) of the sputtered CrCoCuFeNi thin films

The multifractal spectrum, f(α), plotted against the singularity exponent (α) (Figure 7) is an indication of the surface dynamics during thin film growth. As shown, the profiles are humped and strongly skewed to the right, which implies that these surfaces are multifractal. The spatial complexity of the surfaces is determined by the right shifts of the profiles, i.e. in this case, samples prepared at high temperatures, generally, have their profiles strongly shifting to the right whereas those prepared at low temperatures to the left. This is a confirmation of the increase in lateral complexity of the films with increasing deposition temperature. In addition, the multifractal spectrum indicates the evolution characteristics of the thin film surfaces during deposition, and as such, high temperature leads to coalescence and formation of complex surface structures. The multifractal measures obtained from Figure 7 are shown in Table 4. The highest peak of the spectrum (f_{max}) can be observed for samples B and D, which further confirms the multifractal strength of these samples and the strong influence of the deposition temperature on the spatial growth of HEAs thin films during a sputtering process. The width of the spectrum, Δf(α), for all the samples is positive, indicating that the distribution of the surface structures depends on the maximum subset probability. Sample D has the lowest value of Δf(α), which indicates that it has the smallest maximum peaks as compared to the rest; this agrees with the fractal and statistical results. Large values of Δα are an indication of high lateral growth and non-uniform distribution of structures. In this case, samples prepared at high substrate temperature and sputtering power are seen to exhibit larger values of Δα. It, therefore, indicates that high power and substrate temperature contribute to the lateral evolution of the thin film structures during sputtering.

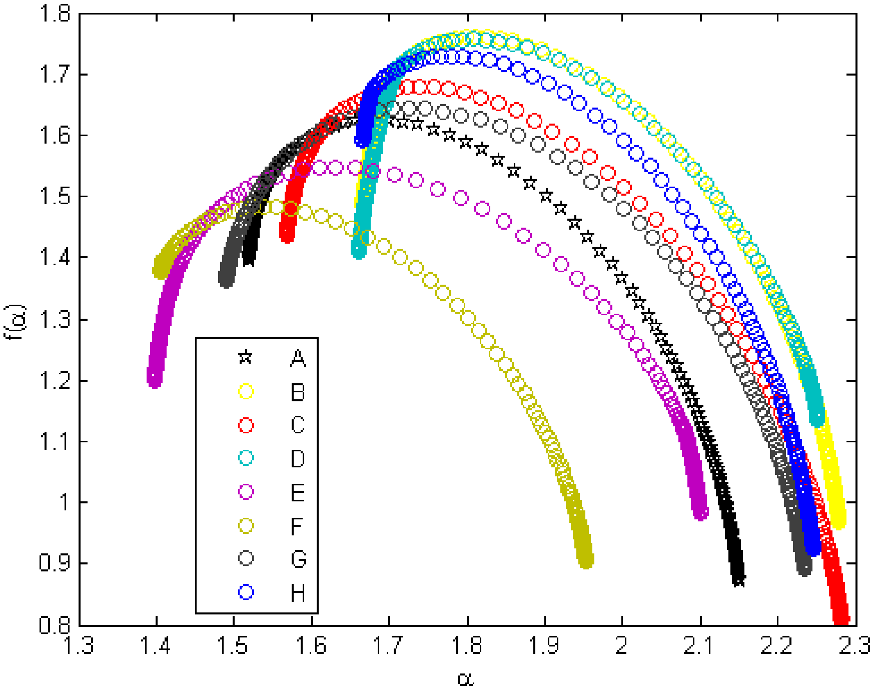

Figure 7. Multifractal spectra of the sputtered CrCoCuFeNi thin films

Table 3 Fractal parameters of the sputtered CrCoCuFeNi thin films. All the values of D have an error of ±0.01

Parameter	**A**	**B**	**C**	**D**	**E**	**F**	**G**	**H**
Fractal dimension (D_f)	1.699	1.783	1.732	1.781	1.590	1.659	1.693	1.773
Lacunarity coefficient	0.082	0.048	0.036	0.051	0.121	0.108	0.128	0.041

Table 4 Multifractal spectrum measures of the sputtered CrCoCuFeNi thin films

Samples	α_{min}	α_{max}	$\Delta\alpha$	f_{min}	f_{max}	Δf
A	1.49	2.151	0.661	0.873	1.704	0.831
B	1.653	2.279	0.626	0.9671	1.758	0.7909
C	1.529	2.282	0.753	0.8089	1.727	0.9181
D	1.638	2.251	0.613	1.134	1.757	0.623
E	1.397	2.100	0.703	0.983	1.636	0.653
F	1.405	1.953	0.548	0.9034	1.545	0.6416
G	1.490	2.235	0.745	0.8919	1.724	0.8321
H	1.666	2.246	0.58	0.925	1.730	0.805

4 Conclusions

High entropy thin films of CrCuCuFeNi prepared through radiofrequency magnetron sputtering have been studied through nanoscale dynamic analysis in this article. The thin films were sputtered at different deposition times, substrate temperature, and radiofrequency sputtering power and their topographies were obtained via the AFM method. It was demonstrated that the surface roughness (average and interface width) decreases with the deposition time. It was also shown that the influence of the sputtering power cannot be predicted through the statistical approach rather than the fractal analysis. It was shown that higher sputtering power leads to spatial complex evolution during the sputtering of these films. The autocorrelation functions, for all samples, exhibit exponential decrease and at high substrate temperature and sputtering power, there is the formation of mounded surfaces, which is attributed to structural clustering. The height-height correlation function exhibit two regimes (linear and oscillatory regimes), which are typical characteristics of fractal surfaces. The spatial evolution of surfaces during sputtering, as depicted by the fractal dimension, determines the homogeneity of the thin film structures as demonstrated by the coefficients of lacunarity. The generalized fractal dimension and mass exponent against the moment orders are indications of self-affine surfaces whereas the multifractal spectrum measures indicated that the surfaces were multifractals. It was observed that samples prepared at high substrate temperature and power are strongly multifractal and therefore, this study concludes that the surface roughness and spatial evolution of high entropy thin films of CrCoCuFeNi are strongly influenced by the deposition temperature, sputtering power and insignificantly by deposition time.

5 References

[1] K. Huang, G. Wang, H. Qing, Y. Chen, and H. Guo, “Effect of Cu content on electrical resistivity, mechanical properties and corrosion resistance of AlCu NiTiZr0.75 high entropy alloy films,” *Vacuum*, vol. 195, no. August 2021, p. 110695, Jan. 2022, doi: 10.1016/j.vacuum.2021.110695.

[2] K.-S. Chang, K.-T. Chen, C.-Y. Hsu, and P.-D. Hong, “Growth (AlCrNbSiTiV)N thin films on the interrupted turning and properties using DCMS and HIPIMS system,” *Appl. Surf. Sci.*, vol. 440, pp. 1–7, May 2018, doi: 10.1016/j.apsusc.2018.01.110.

[3] W. Muftah, J. Allport, and V. Vishnyakov, “Corrosion performance and mechanical properties of FeCrSiNb amorphous equiatomic HEA thin film,” *Surf. Coatings Technol.*, vol. 422, no. May, p. 127486, Sep. 2021, doi: 10.1016/j.surfcoat.2021.127486.

[4] C. Sha, Z. Zhou, Z. Xie, and P. Munroe, “High entropy alloy FeMnNiCoCr coatings: Enhanced hardness and damage-tolerance through a dual-phase structure and nanotwins,” *Surf. Coatings Technol.*, vol. 385, no. February, p. 125435, Mar. 2020, doi: 10.1016/j.surfcoat.2020.125435.

[5] J.-T. Liang *et al.*, “Comparisons of plasma-sprayed and sputtering Al0.5CoCrFeNi2 high-entropy alloy coatings,” *Surf. Coatings Technol.*, vol. 403, no. July, p. 126411, Dec. 2020, doi: 10.1016/j.surfcoat.2020.126411.

[6] N. A. Khan *et al.*, “RF magnetron sputtered AlCoCrCu0.5FeNi high entropy alloy (HEA) thin films with tuned microstructure and chemical composition,” *J. Alloys Compd.*, vol. 836, p. 155348, Sep. 2020, doi: 10.1016/j.jallcom.2020.155348.

[7] C. Sha, Z. Zhou, Z. Xie, and P. Munroe, “FeMnNiCoCr-based high entropy alloy coatings: Effect of nitrogen additions on microstructural development, mechanical properties and tribological performance,” *Appl. Surf. Sci.*, vol. 507, no. November 2019, p. 145101, Mar. 2020, doi: 10.1016/j.apsusc.2019.145101.

[8] J. Wang, S. Kuang, X. Yu, L. Wang, and W. Huang, “Tribo-mechanical properties of CrNbTiMoZr high-entropy alloy film synthesized by direct current magnetron sputtering,” *Surf. Coatings Technol.*, vol. 403, no. July, p. 126374, Dec. 2020, doi: 10.1016/j.surfcoat.2020.126374.

[9] F. M. Mwema, E. T. Akinlabi, O. P. Oladijo, and S. Krishna, “Microstructure and scratch analysis of aluminium thin films sputtered at varying RF power on stainless steel substrates,” *Cogent Eng.*, vol. 7, no. 1, p. 1765687, Jan. 2020, doi: 10.1080/23311916.2020.1765687.

[10] F. M. Mwema, E. T. Akinlabi, O. P. Oladijo, and J. D. Majumdar, “Effect of varying low substrate temperature on sputtered aluminium films,” *Mater. Res. Express*, vol. 6, no. 5, p. 056404, Feb. 2019, doi: 10.1088/2053-1591/ab014a.

[11] O. Abegunde Olayinka, A. Esther, O. P. Oladijo, and J. D. Majumdar, “Surface integrity of TiC thin film produced by RF magnetron sputtering,” *Procedia Manuf.*, vol. 35, pp. 950–955, 2019, doi: 10.1016/j.promfg.2019.06.040.

[12] F. M. Mwema, E. T. Akinlabi, and O. P. Oladijo, “Micromorphology of sputtered aluminum thin films: A fractal analysis,” *Mater. Today Proc.*, vol. 18, pp. 2430–2439, 2019, doi: 10.1016/j.matpr.2019.07.091.

[13] F. M. Mwema, E. T. Akinlabi, O. P. Oladijo, S. A. Akinlabi, and S. Hassan, “A Multifractal Study of Al Thin Films Prepared by RF Magnetron Sputtering,” in *Lecture Notes in Mechanical Engineering*, 2020, pp. 687–694.

[14] D. Nečas and P. Klapetek, “Gwyddion: An open-source software for SPM data analysis,” *Cent. Eur. J. Phys.*, vol. 10, no. 1, pp. 181–188, 2012, doi: 10.2478/s11534-011-0096-2.

[15] Ş. Ţălu, R. S. Matos, E. P. Pinto, S. Rezaee, and M. Mardani, “Stereometric and fractal analysis of sputtered Ag-Cu thin films,” *Surfaces and Interfaces*, vol. 21, no. August, p. 100650, Dec. 2020, doi: 10.1016/j.surfin.2020.100650.

[16] F. M. Mwema, E. T. Akinlabi, and O. P. Oladijo, “Fractal analysis of hillocks: A case of RF sputtered aluminum thin films,” *Appl. Surf. Sci.*, vol. 489, no. May, pp. 614–623, Sep. 2019, doi: 10.1016/j.apsusc.2019.05.340.

[17] Ş. Ţălu, S. Stach, S. Valedbagi, R. Bavadi, S. M. Elahi, and M. Ţălu, “Multifractal characteristics of titanium nitride thin films,” *Mater. Sci.*, vol. 33, no. 3, pp. 541–548, Sep. 2015, doi: 10.1515/msp-2015-0086.

[18] A. Das *et al.*, “Analyzing the surface dynamics of titanium thin films using fractal and multifractal geometry,” *Mater. Today Commun.*, vol. 27, no. December 2020, p. 102385, Jun. 2021, doi: 10.1016/j.mtcomm.2021.102385.

[19] E. S. Gadelmawla, M. M. Koura, T. M. A. Maksoud, I. M. Elewa, and H. H. Soliman, “Roughness parameters,” *J. Mater. Process. Technol.*, vol. 123, no. 1, pp. 133–145, 2002, doi: 10.1016/S0924-0136(02)00060-2.

[20] M. Senthilkumar, N. K. Sahoo, S. Thakur, and R. B. Tokas, “Characterization of microroughness parameters in gadolinium oxide thin films: A study based on extended power spectral density analyses,” *Appl. Surf. Sci.*, vol. 252, no. 5, pp. 1608–1619, 2005, doi: 10.1016/j.apsusc.2005.02.122.

[21] F. M. Mwema, E. T. Akinlabi, and O. P. Oladijo, “Effect of Substrate Type on the Fractal Characteristics of AFM Images of Sputtered Aluminium Thin Films,” *Mater. Sci.*, vol. 26, no. 1, pp. 49–57, Nov. 2019, doi: 10.5755/j01.ms.26.1.22769.

Acknowledgement

Research described in the paper was supported by the Internal Grant Agency of Brno University of Technology, grant No. FEKT-S-20-6352. Part of the work was carried out with the support of CEITEC Nano Research Infrastructure supported by MEYS CR (LM2018110).

University of Johannesburg UJ-GES 4.0 Research fellowship scholarship is also acknowledged.